

# Monitoring of bacterial film formation and its breakdown with an angular-based surface plasmon resonance biosensor†

Cite this: DOI: 10.1039/c7an00068e

 Sandrine Filion-Côté,<sup>a</sup> Ferial Mélaïne,<sup>b</sup> Andrew G. Kirk<sup>a</sup> and Maryam Tabrizian <sup>\*b,c</sup>

Bacterial biofilms are a leading cause of infection in health-care settings. Surface plasmon resonance (SPR) biosensors stand as valuable tools not only for the detection of biological entities and the characterisation of biomaterials but also as a suitable means to monitor bacterial film formation. This article reports on a proof-of-concept study for the use of an angular-based SPR biosensor for the monitoring of bacterial cell growth and biofilm formation and removal under the effect of different cleaning agents. The benefit of this custom-made SPR instrument is that it records simultaneously both the critical and resonant angles. This provides unique information on the growth of bacterial cells which is otherwise not obtainable with commonly used intensity-based SPR systems. The results clearly showed that a multilayer biofilm can be formed in 48 hours and the steps involved can be monitored in real-time with the SPR instrument through the measurement of the refractive index change and following the evolution in the shape of the SPR curve. The number, the depth and the sharpness of the reflection ripples varied as the film became thicker. Simulation results confirmed that the number of layers of bacteria affected the number of ripples at the critical angle. Real-time monitoring of the film breakdown with three cleaning agents indicated that bleach solution at 4.5% was the most effective in disrupting the biofilm from the gold sensor. Our overall findings suggest that the SPR biosensor with angular modulation presented in this article can perform real-time monitoring of biofilm formation and has the potential to be used as a platform to test the efficiency of disinfectants.

Received 12th January 2017,

Accepted 5th May 2017

DOI: 10.1039/c7an00068e

[rsc.li/analyst](http://rsc.li/analyst)

## 1. Introduction

Biofilms are three-dimensional structures composed of microcolonies of microorganisms cocooned in an extracellular matrix of lipids, polysaccharides, proteins and DNA. Several stages are involved in the formation of a biofilm.<sup>1–3</sup> The bacterial cells first adhere on a surface with an initially reversible attachment. They start to secrete an extracellular polymeric substance which attaches them irreversibly to the surface. They then multiply to form microcolonies while still generating and strengthening their extracellular matrix. Once the biofilm is mature, channels within and between microcolonies allow for oxygen and nutrient transport as well as for com-

munication. Bacteria can undergo mutation in this secure structure and eventually release single cells to form a new biofilm elsewhere. Bacterial cells in a biofilm are much stronger and more resistant to their environment, cleaning agents and antibiotics than their planktonic counterparts.<sup>4,5</sup> The protection offered by the extracellular matrix as well as the exchange taking place between bacteria inside this matrix make the bacterial biofilms an important source of infectious diseases in health-care settings.

Proper cleaning of surfaces and medical tools is a key step in reducing the number of infections in hospitals. Various cleaning agents with different action mechanisms are used to eliminate undesirable microorganisms. These agents can be grouped into two categories: detergents and disinfectants. Detergents remove and limit the adhesion of contaminants on surfaces and often require a mechanical action, such as friction, to be efficient. Detergents must be used prior to a disinfectant treatment as they remove organic contaminants that would otherwise reduce the efficiency of the disinfectant. They also increase the contact surface of the disinfectant with the microorganisms.<sup>6</sup> Disinfectants, on the other hand, attack the constituents of the microorganisms, for example proteins and

<sup>a</sup>The Photonic Systems Group, Dept. Electrical and Computer Engineering, McGill University, McConnell Engineering Building, Montréal, H3A 0E9, Canada

<sup>b</sup>Department of Biomedical Engineering, McGill University, Duff Medical Building, Montréal, H3A 2B4, Canada

<sup>c</sup>Faculty of Dentistry, McGill University, Strathcona Anatomy & Dentistry Building, Montréal, H3A 0C7, Canada. E-mail: [maryam.tabrizian@mcgill.ca](mailto:maryam.tabrizian@mcgill.ca)

†Electronic supplementary information (ESI) available. See DOI: 10.1039/c7an00068e

cell membranes, and are divided into a few classes based on their action mechanism. Examples of disinfectants are chlorine (*e.g.* sodium hypochlorite found in common household bleach), alcohols (*e.g.* ethanol), quaternary ammonium compounds (*e.g.* benzalkonium chloride) and oxidizers (*e.g.* hydrogen peroxide).<sup>6,7</sup>

Current methods to investigate biofilm formation include plate counting complemented by fluorescence of metabolic indicators, confocal scanning laser microscopy, atomic force microscopy and scanning electron microscopy.<sup>8</sup> Similarly, to assess the efficiency of a disinfectant, the most commonly used method is also plate counting before and after exposure of the bacteria to a disinfectant. This method comprises multiple steps and the required manipulation of the biofilm can alter the results. In the last few decades, surface plasmon resonance (SPR) has emerged as a sensitive technique for a wide range of sensing applications including the detection of proteins, DNA and other biological components at very low concentration,<sup>9–11</sup> the characterisation of biomaterials,<sup>12</sup> and more recently, for the detection and monitoring of whole cells.<sup>13–16</sup> This optical technique consists of measuring the intensity of the light reflecting from a thin metal film through a glass prism as a function of the incident angle. Its high sensitivity is linked to the variation in resonance conditions that can be observed for small bulk or surface refractive index changes of the sample adjacent to the metal. However, the intensity-based SPR biosensors are unable to instantaneously capture the entire angular SPR curve. This may be required in some situations such as bacterial growth and formation of biofilms. Herein, a custom-made surface plasmon resonance biosensor that simultaneously records both the critical and resonant angles was used to acquire information on the growth of bacterial cells and biofilm formation in real-time. We demonstrated the capabilities of this angular-based biosensor not only for monitoring the whole biofilm formation process from the attachment of bacterial cells to its maturation but also its

suitability as a platform to test cleaning agents for bacterial film removal by following their actions as they occur.

## 2. Materials and methods

### 2.1 Surface plasmon resonance biosensor

The details of the SPR instrument along with the corresponding data analysis method were reported in a paper published previously by the authors.<sup>18</sup> Briefly, the biosensor consists of a collimated light emitting diode (LED) source centered at 630 nm, a polariser, a 50 mm cylindrical lens, an SF11 equilateral prism, another 50 mm cylindrical lens and a camera (Fig. 1). The polariser is oriented to ensure TM polarisation is incident on the gold and the lenses generate an angular range of 10 degrees centered at 53°. The use of a cylindrical lens allows us to capture at once the whole SPR curve including both the critical and resonant angles.

The instrument operates in real-time where an angular SPR curve (reflectivity *versus* incident angle) is captured on the camera. The two significant locations of an SPR curve are the critical angle and the resonant angle. The critical angle is characterised by a sharp inflection on the left-hand side of the SPR curve and is where total internal reflection occurs while the resonant angle is where the reflectivity is at its minimum (Fig. 1). Using the SPR curve, the effective refractive index of the medium above the sensing surface is calculated through a projection method in Matlab.<sup>19,20</sup> In this method, the measured SPR reflection spectrum is expressed as a column vector  $\mathbf{v}$  with one element for each camera pixel. In advance of the experimental measurement, a rectangular matrix  $\mathbf{A}$  is calculated in which each row corresponds to the simulated reflectivity for a given refractive index within the dynamic range of the instrument. The inner product  $\mathbf{A} \cdot \mathbf{v}$  results in a column vector  $\mathbf{s}$  which has one value for each simulated refractive index. By interpolating over  $\mathbf{s}$  to find the refractive index value

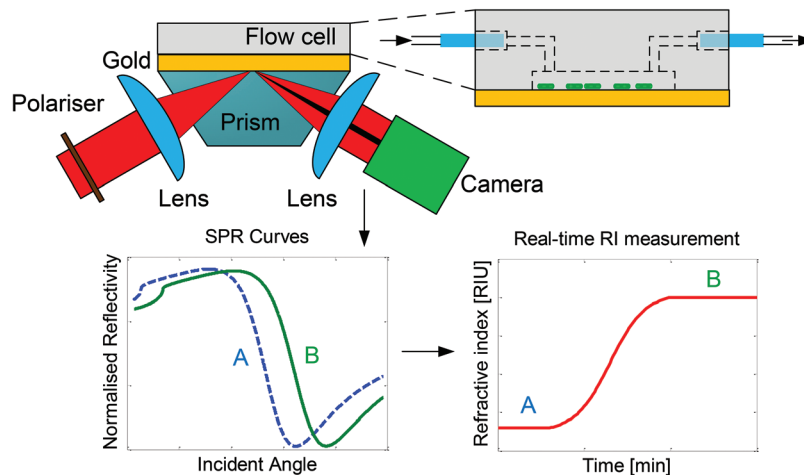


**Fig. 1** SPR instrument with angular modulation mounted with a microfluidic flow cell. The source is a collimated LED centered at 630 nm and the polariser maintains TM polarisation. The cylindrical lenses generate the angular spectrum for the SPR curves captured by the camera. These curves are then analysed for the measurement of the refractive index of a sample in real-time.

where  $s$  is a maximum, the refractive index that most closely matches  $v$  is obtained. Changes in the refractive index below  $1 \times 10^{-6}$  refractive index units (RIU) have been measured using this method.<sup>20</sup>

## 2.2 Gold coated glass

The sensing surface was an SF11 glass slide coated with 2 nm of chromium and 40 nm of gold (Sydor Optics). Before each measurement in the SPR instrument, the coated glass was cleaned by soaking it in acetone and isopropanol for one minute each and by rinsing it in distilled water. The coated glass was dried with compressed air.

## 2.3 Preparation of bacterial cell samples & buffer solution

The buffer was a mixture of 30% Luria–Bertani (LB) growth medium (Fisher Biotech: LB Broth, Lennox (powder), Fisher Scientific, Fair Lawn, New Jersey, USA) with serum, an isotonic solution with a concentration of 9 g of NaCl per litre of water. For the bacterial cell samples, 10  $\mu$ l of stock solutions of *Escherichia coli* DH5 $\alpha$  was inoculated in 3 ml of LB broth and placed in an incubator at 37 °C with shaking (250 RMP) for 17 hours. The bacterial cells were centrifuged and re-suspended in serum three times to wash away the growth medium. The initial concentration was defined by the total number of bacteria in one ml of serum and it was calculated every time in serial dilution and plate counting. A ten-fold dilution of this initial concentration was used for the experiments and the resulting concentration of the sample was around  $2 \times 10^8$  cfu ml<sup>-1</sup>.

## 2.4 Disinfectants & detergents

Three cleaning agents were used for the biofilm removal efficiency tests: Bleach LAVO PRO6 (LAVO Inc., Montréal, Canada) diluted to 4.5% in MilliQ water, anhydrous ethyl alcohol (Commercial Alcohols, Ontario, Canada) diluted to 70% and Versa-Clean multi-purpose cleaner (Fisherbrand, Fisher Scientific, Nepean, Ontario, Canada) diluted to 20%. The biofilm removal experiments were performed with cleaning agent concentrations in the order recommended by the manufacturers.

## 2.5 Experimental conditions

The experiments were conducted at room temperature and with no prior surface chemistry. First, the flow cell and microfluidic circuit were cleaned with 70% ethanol for 20 minutes and rinsed with sterile water. The buffer was then introduced at a flow rate of 26.8  $\mu$ l min<sup>-1</sup> and the SPR response was left to stabilize for an hour. This flow rate was retained throughout the entire experiment. The bacterial sample was injected through a 1200  $\mu$ l injection loop and left to adhere and to grow on the gold surface.

The flow cell used on the sensing surface had two chambers that allowed for the simultaneous measurement of the refractive indices of both the growing bacteria on the gold surface and of the reference bare gold surface. This helped decipher between changes occurring on the bacterial film and

a simple change in the refractive index resulting from a change of buffer.

## 2.6 Micrographs of bacterial cells on gold

The bacterial cells were grown on the sensing surface for one, 20 and 48 hours (using a different gold sensor and a new bacterial sample for each time point) under the conditions described in section 2.5. Afterwards, the gold sensor was removed without disturbing the bacteria layer and was placed under a microscope (WITec Alpha300RS, Germany). Images were captured with a 20 $\times$  objective lens.

## 2.7 SPR monitoring of bacterial attachment and removal

For the biofilm formation experiments, the growth of the bacterial cells was monitored for three days under the conditions described in section 2.5.

For the disinfectant tests, the bacteria grew on the sensing surface for 48 hours. The buffer was replaced with sterile water to halt the bacterial growth. Once the signal stabilized, the disinfectant was injected through a 600  $\mu$ l injection loop. At the end of each biofilm removal assay, the sensing surface was cleaned by injecting a 20% bleach solution, was then removed from the instrument and cleaned again with the procedure described in section 2.2 for reuse in the next experiments. The biofilm removal assay was repeated three times for each cleaning agent.

# 3. Results & discussion

## 3.1 Real-time monitoring of bacterial cell attachment and growth on gold

A flow rate of 26.8  $\mu$ l min<sup>-1</sup> was used to inject a bacterial sample in the flow cell adjacent to the gold surface. Fig. 2 shows the attachment and the growth of bacterial cells. The inset illustrates distinct transitions in the refractive index upon the bacterial injection and attachment. Initially, the refractive index corresponds to the buffer on the bare gold. The first increase indicates the change in the refractive index caused by the suspended bacteria in buffer as soon as they entered the flow cell. The signal then varied as the bacteria started to attach on the gold surface while the amount of bacteria in suspension decreased. Finally, the sample containing unattached bacteria was washed out from the flow cell. In this case, the changes in the refractive index could be only associated with the attached bacterial cells that were starting to grow on the sensing surface in buffer media. The difference in the refractive index value between the baseline and the post-injection signal then was regarded as an indication of the bacterial attachment on the sensor.

The refractive index signal was monitored during three days under continuous buffer flow made of 30% LB in serum running at a rate of 26.8  $\mu$ l min<sup>-1</sup>. The refractive index increased substantially with respect to the baseline but also slowly fluctuated over time. The refractive index calculated with the projection method<sup>20</sup> was mostly influenced by the

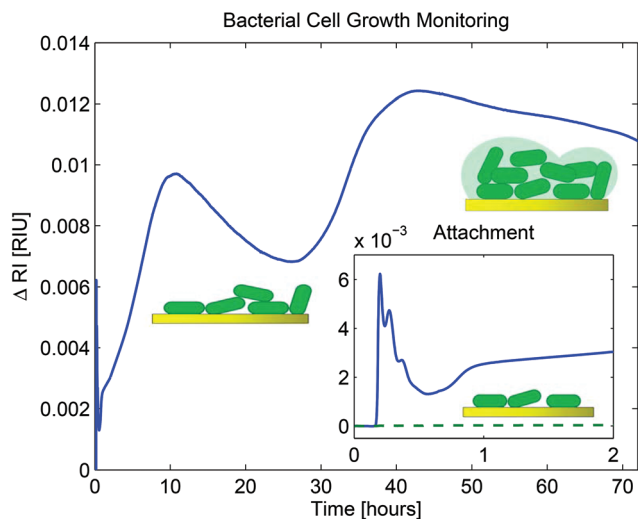


**Fig. 2** Real-time refractive index monitoring for bacterial cell growth over three days. The refractive index varies over time with the formation of a biofilm which implies the multiplication of bacterial cells and the fluctuation in the surface coverage. The data shown is normalised with the simultaneous measurement on bare gold. Inset: Real-time monitoring of the injection of bacterial cells and their subsequent attachment on the gold surface in the SPR instrument. The bacterial cell sample was in the flow cell between times 0.2 and 0.8 hours (10 and 50 minutes). The variations in the refractive index observed in this time interval correspond to bulk changes. For the following hour, the increase in the signal shows the bacteria attached on the gold surface (solid line) starting to grow while the refractive index on the bare gold surface remains unchanged (dotted line).

location of the resonant angle. Since bacteria are thicker than the sensing region of the plasmon (around 200 nm), the resonant angle only responds to the first layer of bacteria, *i.e.*, the cell envelope and part of the cytoplasm.<sup>21</sup> The refractive index measured over time was therefore an effective refractive index resulting from the cytoplasm of the bacteria, their secretions and the buffer. Fig. 2 shows the monitoring of the refractive index as the bacterial cells grew on the gold surface and built their biofilm. The refractive index initially increased largely due to the multiplication of bacteria on the surface. The bacteria then reached a certain growth level where they started to produce their extracellular matrix, form micro-colonies and re-organised their structure into a biofilm. The steps in the formation of a biofilm involve a variation in the surface coverage<sup>22</sup> that is believed to induce the fluctuation of the refractive index observed over time, particularly, the decrease and following increase around 25 hours. The multiplication of bacterial cells and the secretion of their extracellular matrix generate an increase in the refractive index measured at the surface. On the other hand, only the expected shift in surface coverage upon the formation of the biofilm accounts for a decrease in the signal. Since a biofilm is mostly composed of the extracellular matrix with the bacteria representing a lower percentage,<sup>22</sup> the generation of the extracellular polymeric substance contributed to the change in the refractive index with an increase in the bulk refractive index in

the surrounding of the bacteria by slowly dominating the space previously occupied by the buffer. The result shown in Fig. 2 was repeated over a dozen times with the same outcomes in the variation of the refractive index over time.

Interesting results were obtained from the modification in shape and position of the SPR curve during bacterial growth. The SPR curve is the reflected intensity on the gold sensor as a function of the incident angle. The two important locations on this curve are the critical angle where total internal reflection occurs (around 49°) and the resonant angle at minimum intensity (around 55°). As the bacteria multiplied and built more

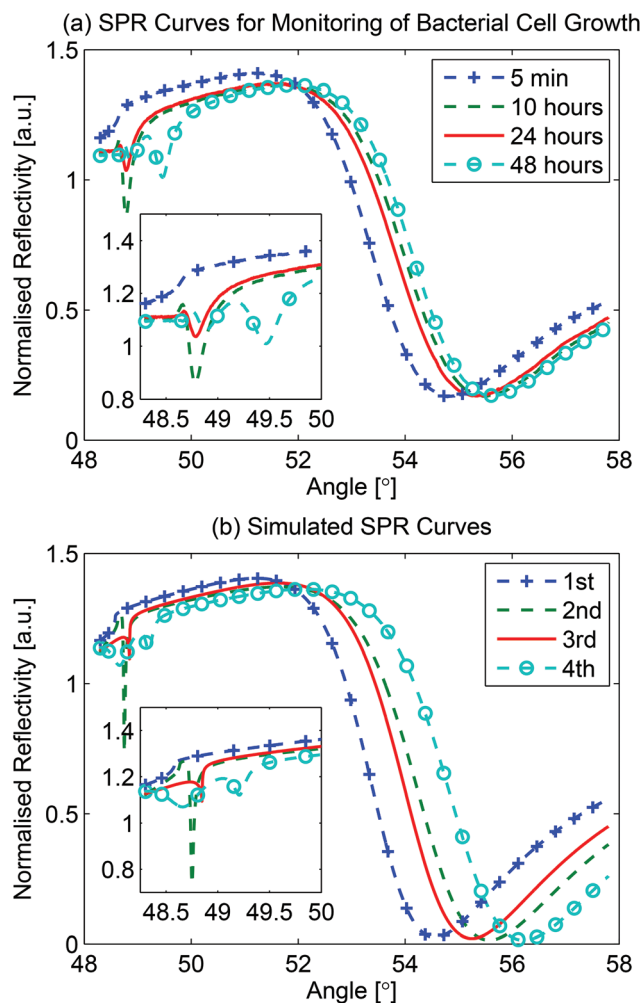


**Fig. 3** (a) Experimental SPR curves at different stages of the bacterial film formation. 5 min: SPR curve for buffer, before the attachment of bacteria. 10 hours: the bacterial cells multiplied and built a few layers. 24 hours: the bulk refractive index increased with the secretion of the extracellular polymeric substance. 48 hours: a few more layers were added to the biofilm structure and the extracellular matrix is in place. Inset: Close-up at the critical angle. (b) Simulated SPR curves. 1st: no bacteria and bulk refractive index of 1.334. 2nd: 4 layers of bacteria (film thickness of 2.2  $\mu\text{m}$  and refractive index of 1.34), 70% of coverage and bulk refractive index of 1.335. 3rd: 4 layers of bacteria, 30% of coverage and bulk refractive index of 1.3395. 4th: 6 layers of bacteria (film thickness of 3.3  $\mu\text{m}$ ), 80% of coverage and bulk refractive index of 1.37. Inset: Close-up at the critical angle. Note: An *E. coli* cell has a diameter of about 1  $\mu\text{m}$ , a length of 2  $\mu\text{m}$ , and a volume of 1  $\mu\text{m}^3$ .

layers, it generated clear features on the SPR curve around the critical angle. The position of the resonant angle depends only on the surface changes since the evanescent wave of the surface plasmon only penetrates the first 200 nm of the sample. The features at the critical angle on the other hand, are influenced by the entire multi-layer structure on the sensing surface while its location depends on the bulk refractive index. Fig. 3(a) shows the evolution of the experimental SPR curves with bacterial cell growth over time. A recording of the SPR curves in real-time is also available in the ESI (Video S1†). Initially, the curve was typical with a sharp inflection at the critical angle. During the formation of the biofilm, the shape of the curve in that region was altered, and ripples appeared. The number, the depth and the sharpness of the ripples varied as the film became thicker. Simulation results obtained with Matlab confirmed that the thickness of the biofilm, representing an increasing number of layers of bacteria, affected the number of ripples at the critical angle (Fig. 3(b)). They also showed that the depth and sharpness of

the ripples were affected by the refractive index of the surrounding medium with respect to the refractive index of the bacteria. These simulations consisted of generating an SPR curve through the transfer matrix method where the sample is represented by a multi-layer system. While experimentally the sample is not uniform, the simulations were performed with defined layers of chosen refractive indices. The bacteria were simulated with a refractive index of 1.340 for their cytoplasm and the thickness of the film was varied by taking into account an *E. coli* cell diameter around 1  $\mu\text{m}$ . Also, the bulk refractive index was varied from 1.334 to 1.370. When the bulk refractive index was lower than that of the cytoplasm, the ripples were deep and sharp. As the bulk refractive index value converged towards the refractive index of the cytoplasm, the ripples almost disappeared. They reappeared and became deeper as the bulk refractive index exceeded the one of the cytoplasm and continued to increase. Since the shape of the experimental SPR curve observed over time confirmed an increase in the bulk refractive index and the buffer was not changed during the growth, this

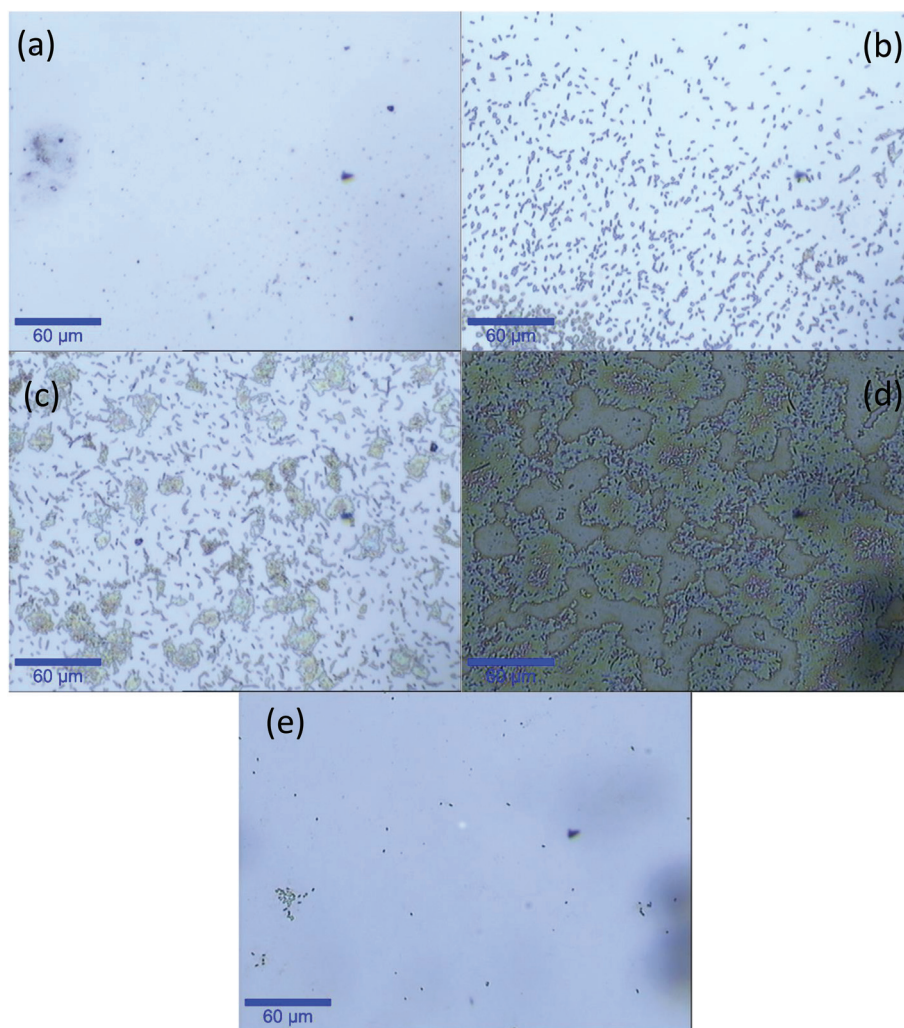


**Fig. 4** Micrographs of bacterial cell growth as a function of time. (a) Bare gold. (b) 1 hour. (c) 20 hours. (d) 48 hours. (e) Surface irrigated with 20% bleach. The magnification is 20 $\times$ .

increase thus indicated the secretion of the extracellular matrix and the formation of the biofilm. The location and shape of the critical angle therefore offer key information about the multi-layer systems on the sensing surface.

### 3.2 Microscopic analysis of surface coverage by bacteria

To validate the SPR results, the surface coverage on the gold sensors at different stages in the growth of bacteria in the SPR biosensor was analysed by light microscopy after one hour, 20 hours and 48 hours of growth in the SPR instrument. As it can be seen in Fig. 4a, b, c and d respectively, after one hour, a few isolated bacteria were attached on gold. After 20 hours, clusters of bacteria started to form while single bacteria were still visible. After 48 hours, bacteria showed the feature of microcolonies. The forming units were no longer apparent since they were wrapped in their extracellular matrix. Once the surface was irrigated with 20% bleach, the biofilm was removed and the surface could be regenerated.

Using image processing functions in Matlab and separating the bacteria from the background through an intensity threshold, the surface coverages were estimated at 14%, 43% and 62% for one, 20 and 48 hours, corresponding to refractive index changes of  $3.5 \times 10^{-3}$ ,  $7.0 \times 10^{-3}$  and  $9.8 \times 10^{-3}$  RIU respectively. Once the bacterial growth reached confluence, the extra layers of bacteria started to form.

### 3.3 SPR biosensor as a platform for testing disinfectants and detergents efficiency for biofilm breakdown

Three cleaning agents, namely bleach (solution of sodium hypochlorite), ethanol and soap (multi-purpose cleaner) were used to monitor the degeneration of the formed biofilm on the SPR sensor. The first two are disinfectants with different action mechanisms as compared to soap which is a detergent. The chlorine ion of sodium hypochlorite attacks the cytoplasmic membrane. Alcohol, on the other hand, denatures proteins.<sup>6</sup> Each agent was diluted to its recommended value. For bleach and soap, the dilution ratios were 4.5% and 20% respectively. For ethanol, the common 70% dilution was used.<sup>23–25</sup> Sterile water and 20% bleach were the negative and positive controls respectively. Fig. 5 shows the effect of the negative and positive controls on the SPR signal after three days of growth. In the case of water, the SPR curve was slightly displaced due to the change in the refractive index. This variation in the refractive index is due to two phenomena: the first is the difference in the refractive index between the buffer and water at the surface since the bacterial film is not uniform and the second is the change in morphology experienced by the bacteria due to the change in salt osmolarity.<sup>13,26,27</sup> This second effect is emphasized by the comparison of the signals of the bacterial film and bare gold in Fig. 5(b). Indeed, if the surface coverage of the bacterial film had not changed, the variation in the refractive index should have been at most as large as the signal shift on bare gold which was only caused by the replacement of the buffer with water. The refractive index for the bacterial film and its surrounding is therefore an effective refractive index. Since the resulting variation in the refractive index was greater for the

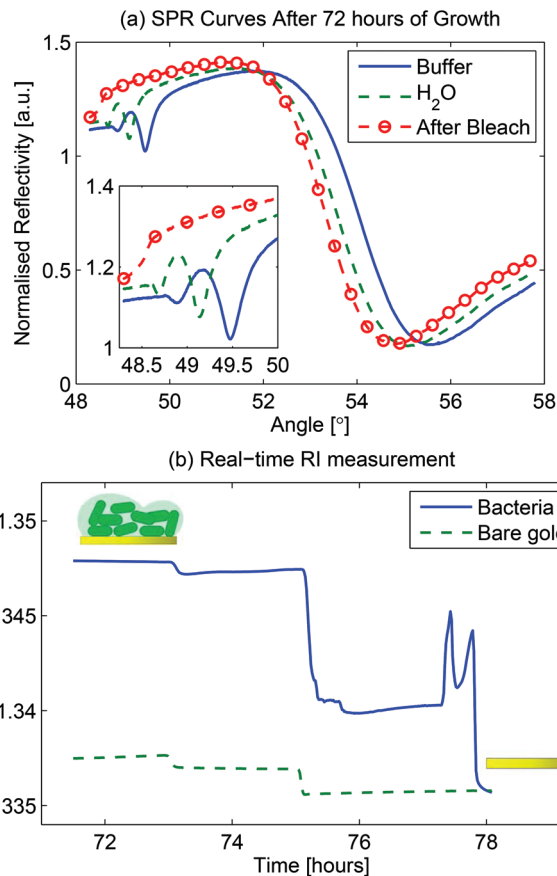


Fig. 5 (a) Experimental SPR curves after three days of bacterial growth in buffer, in water and after being exposed to 20% bleach. The shape of the curve at the critical angle remains the same when the buffer is replaced by sterile water indicating that the bacterial film is still present on the sensing surface. The variation in the depth of the ripples and the shift of both the critical and resonant angles are expected responses to a change in bulk refractive index. Bleach at a concentration of 20% completely eliminates the bacterial film and the SPR curve returns to its original shape and position for bare gold. Inset: Close-up at the critical angle. (b) Refractive index measurements at the end of three days of growth. The bacterial film was initially in growth medium and serum solution. The buffer was replaced by serum at 73 hours and then by water at 75 hours. These changes are visible on both the bacterial film and the bare gold. The greater shift for the bacterial film in water indicates a change in surface coverage. At the end, the bacterial film was exposed to an injection of 20% bleach and the signal returned to baseline confirming that the sensing surface was regenerated.

bacterial film than the bare gold, one can conclude that the surface coverage must have changed with the replacement of buffer with water. However, the bacterial layers, assessable by the shape of the critical angle, clearly remained unaffected by the change of buffer to water. For 20% bleach, the features at the critical angle of the SPR curve corresponding to the bacterial film disappeared, the curve returned to its initial shape and the refractive index decreased to baseline. These observations confirmed that the bacterial film had been removed. A recording of the effect of bleach on the SPR curves in real-time is available in the ESI (Video S2†). It should be noted that the observed

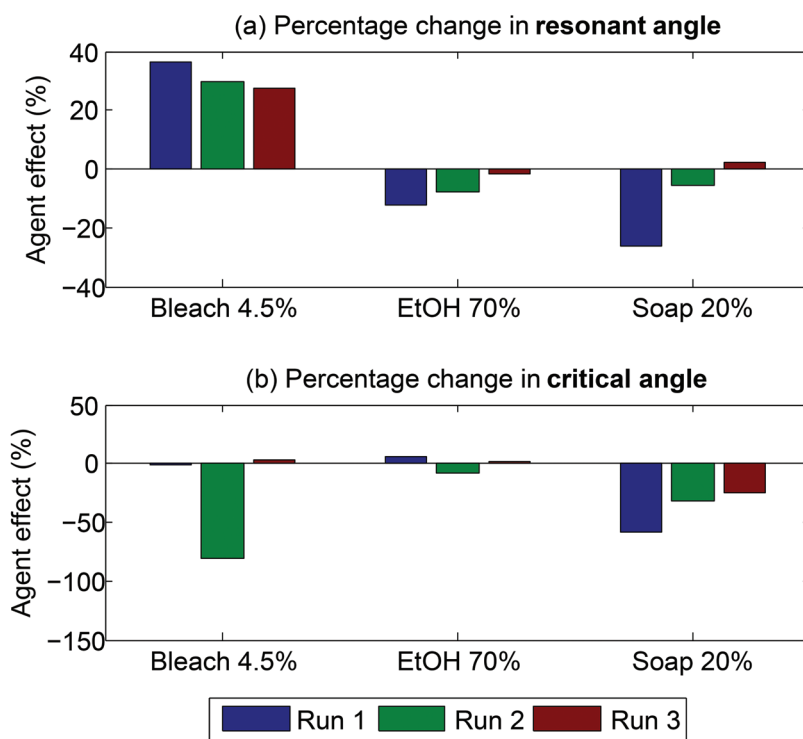
changes in the SPR curve was not due to the alteration of the gold surface; it was verified experimentally that the cleaning agents did not affect the quality and the characteristics of the gold sensing surface (Fig. S4†).

Fig. 6 shows the effect of the three cleaning agents on bacterial films. The ratio in percentage of the refractive index change before and after the exposure of the biofilm to the cleaning agent ( $\Delta RI_{\text{agent}}$ ) and the change in the refractive index resulting from the 48-hour growth of the biofilm with respect to the buffer baseline ( $\Delta RI_{\text{growth}}$ ) can be calculated using eqn (1):

$$\Delta\% = \frac{\Delta RI_{\text{agent}}}{\Delta RI_{\text{growth}}} \times 100 \quad (1)$$

The change in the surface refractive index reflected by the variation at the resonant angle was first calculated using the

whole SPR curve. The change in the bulk refractive index was also estimated using only the total internal reflection section of the SPR curve. This change was associated with the variation at the critical angle caused mainly by the thickness of the biofilm. The difference in the refractive index of the cleaning agent with respect to the buffer did not affect this calculation, since the refractive index was measured before and after the exposure to the cleaning agent under the same buffer conditions. In the case of 70% ethanol, the signal both at the critical and the resonant angles barely changed after the bacterial film exposure to the disinfectant suggesting that the layers of bacteria were unaffected by the product and remained on the surface. This could be due to the high hydrophobicity of biofilms in ethanol solutions as was demonstrated by Epstein *et al.*<sup>28</sup> The hydrophobicity would minimise the contact of the



(c) Summary of percentage change at resonant ( $\theta_R$ ) and critical ( $\theta_C$ ) angles

	Bleach		Ethanol		Soap	
	$\theta_R$	$\theta_C$	$\theta_R$	$\theta_C$	$\theta_R$	$\theta_C$
Run 1	36.3	-0.4	-12.0	5.7	-26.4	-58.4
Run 2	29.7	-81.1	-7.9	-8.3	-5.9	-32.4
Run 3	27.6	3.8	-1.5	1.3	2.3	-24.2
Average	$31.2 \pm 4.6$	$-25.9 \pm 47.9$	$-7.1 \pm 5.3$	$-0.4 \pm 7.1$	$-10.0 \pm 14.8$	$-38.3 \pm 17.9$

**Fig. 6** Effect of cleaning agents on the bacterial films after 48 hours of growth. (a) Effect on the surface refractive index through the resonant angle and (b) effect on the bulk refractive index through the critical angle. The response is expressed with the percent variation in the refractive index calculated with eqn (1); positive values mean the refractive index at the surface increased with the exposure of the biofilm to the cleaning agent while negative values represent a decrease. Each group of three bars is for a different cleaning agent (bleach, ethanol and soap) and each bar is a different run. These results showed that bleach solution at 4.5% was the most effective in disrupting the biofilm on the gold sensor despite its large run-to-run variation. (c) Summary of effect of cleaning agents at resonant and critical angles with average and standard deviation.

1 disinfectant with the biofilm and prevent it from affecting the  
bacteria. For the soap solution, the features displayed at  
the critical angle of the SPR curve revealed a change in the  
structure of the bacterial film. This feature in the SPR curve at  
5 the critical angle suggested that in all three runs with this  
detergent, a few layers of bacteria were removed while some  
were still present on the gold surface. The small changes at the  
resonant angle also indicated variation in the surface coverage  
and/or removal of some of the extracellular matrix. The results  
10 with 4.5% bleach showed run-to-run variations regarding the  
elimination of the bacterial film. In all three runs, the surface  
refractive index increased. A possible explanation of this effect  
is the death of the remaining bacterial cells. A distinction  
15 between killing and removing a biofilm with bleach was dis-  
cussed by Gomes *et al.*<sup>29</sup> Their results showed that bleach  
could kill sessile bacteria while they remained adherent to the  
surface. This would explain the experimental results observed  
where the refractive index increased with the alteration of the  
20 bacterial cells that remained in the biofilm. The experimental  
SPR curves for before and after the exposure of the bacterial  
films to the three cleaning agents are available in the ESI  
(Fig. S3†). The changes in the shape of the critical angle  
were used in combination with the change in the refractive  
25 index measured through the location of the resonant angle to  
evaluate the effect of the cleaning agents. The abrupt and fast  
changes in the SPR curve that occurred from the exposure of  
the biofilm to the disinfectants and detergent were different  
from the more gradual and smooth changes observed during a  
30 change in surface coverage. Thus the two phenomena could be  
differentiated.

## 35 4. Conclusion

The results presented in this work demonstrate that a surface  
plasmon resonance biosensor with simultaneous capture of  
the entire angular spectrum can be used to monitor the forma-  
tion of bacterial biofilms over 48 hours and to determine  
40 the effect of cleaning agents on the biofilm removal. The  
advantage of this instrument is its capture of the entire SPR  
curve at once that permits the measurement of the refractive  
index change during the growth of bacterial cells using the  
location of the resonant angle while the shape of the critical  
45 angle supplies crucial information on the steps involved in the  
formation of a biofilm which would not be possible with a tra-  
ditional SPR imaging system or with many other existing tech-  
niques. The three tested cleaning agents, bleach, ethanol and  
a multipurpose soap showed varying efficiency towards biofilm  
50 removal formed after 48 hours when  $2 \times 10^8$  cfu ml<sup>-1</sup> of *E. coli*  
DH5 $\alpha$  was introduced into the SPR flow chamber. We therefore  
believe that the proposed SPR system could be employed to  
test various bacterial growth conditions and validate growth  
55 inhibitors. Its applications could also be extended to the  
characterisation of biomaterials and develop new means to  
prevent the attachment of bacteria or the formation of biofilm  
on medical devices.

## Acknowledgements

The authors gratefully acknowledge support from NSERC  
(Postgraduate scholarships and Strategic Grant in collabora-  
5 tion with Magnus Chemicals Inc. (Boucherville, Canada)) and  
G enome Qu ebec.

## References

- 1 S. Satpathy, S. KumarSen, S. Pattanaik and S. Raut, Review  
on bacterial biofilm: An universal cause of contamination,  
*Biocatal. Agric. Biotechnol.*, 2016, **7**, 56–66.
- 2 M. Kostakioti, M. Hadjifrangiskou and S. Hultgren,  
Bacterial biofilms: development, dispersal, and therapeutic  
15 strategies in the dawn of the postantibiotic era., *Cold Spring  
Harbor Perspect. Med.*, 2013, **3**(4), a010306.
- 3 J. D. Bryers and B. D. Ratner, Bioinspired Implant  
Materials Befuddle Bacteria, *American Society for  
20 Microbiology News*, 2004, **70**(5), 232–237.
- 4 M. E. Olson, H. Ceri, D. W. Morck, A. G. Buret and  
R. R. Read, Biofilm bacteria: formation and comparative  
susceptibility to antibiotics, *Can. J. Vet. Res.*, 2002, **66**, 86–  
92.
- 5 N. H oiby, T. Bjarnsholt, M. Givskov, S. Molin and  
O. Ciofu, Antibiotic resistance of bacterial biofilms,  
*Int. J. Antimicrob. Agents*, 2010, **35**, 322–332.
- 6 R. Massicotte, *D esinfectants et d esinfection en hygi ene et  
salubrit e: Principes fondamentaux*, Qu ebec, 2009.
- 7 W. A. Rutala and D. J. Weber and T. H. I. C. P. A. C.  
(HICPAC), *Guideline for Disinfection and Sterilization in  
30 Healthcare Facilities*, Chapel Hill, 2008.
- 8 D. Lindsay and A. von Holy, Bacterial biofilms within the  
clinical setting: what healthcare professionals should  
35 know, *J. Hosp. Infect.*, 2006, **64**, 313–325.
- 9 J. Homola, Surface Plasmon Resonance Sensors for  
Detection of Chemical and Biological Species, *Chem. Rev.*,  
2008, **108**(2), 462–493.
- 10 T. Xue, X. Cui, W. Guan, Q. Wang, C. Liu and H. Wang,  
Surface plasmon resonance technique for directly probing  
40 the interaction of DNA and graphene oxide and ultra-sensi-  
tive biosensing, *Biosens. Bioelectron.*, 2014, **58**, 374–379.
- 11 T. Riedel, F. Surman, S. Hageneder, O. Pop-Georgievski,  
C. Noehammer, M. Hofner, E. Brynda, C. Rodriguez-  
Emmenegger and J. Dost alek, Hepatitis B plasmonic bio-  
45 sensor for the analysis of clinical serum samples, *Biosens.  
Bioelectron.*, 2016, **85**, 272–279.
- 12 Y. Arima, M. Toda and H. Iwata, Surface plasmon reso-  
nance in monitoring of complement activation on biomateri-  
50 als, *Adv. Drug Delivery Rev.*, 2011, **63**(12), 988–999.
- 13 V. Chabot, Y. Miron, M. Grandbois and P. G. Charette,  
Long range surface plasmon resonance for increased sensi-  
55 tivity in living cell biosensing through greater probing  
depth, *Sens. Actuators, B*, 2012, **174**, 94–101.
- 14 H. Vaisocherov a-L isalov a, I. V iřov a, M. L. Ermini,  
T. řpringer, X. C. Song, J. Mr azek, J. Lama ov a, N. S. Lynn

- 1 Jr., P. Šedivák and J. Homola, Low-fouling surface plasmon resonance biosensor for multi-step detection of foodborne bacterial pathogens in complex food samples, *Biosens. Bioelectron.*, 2016, **80**, 84–90.
- 5 15 P. N. Abadian, N. Tandogan, J. J. Jamieson and E. D. Goluch, Using surface plasmon resonance imaging to study bacterial biofilms, *Biomicrofluidics*, 2014, **8**(2), 02180.
- 10 16 Y. Yuan, T. Guo, X. Qiu, J. Tang, Y. Huang, L. Zhuang, S. Zhou, Z. Li, B. Guan, X. Zhang and J. Albert, Electrochemical surface Plasmon resonance fiberoptic sensor: in-situ detection of electroactive biofilms, *Anal. Chem.*, 2016, **88**(15), 7609–7616.
- 15 17 S. Fillion-Côté, M. Tabrizian and A. G. Kirk, Surface Plasmon Resonance Biosensor as a Tool for the Measurement of Complex Refractive Indices, in *37th Annual International Conference of the IEEE Engineering in Medicine and Biology Society, Milan, Italy*, 2015.
- 20 **Q3** 18 S. Fillion-Côté, M. Tabrizian and A. G. Kirk, Real-time measurement of complex refractive indices with surface plasmon resonance, *Sens. Actuators, B*, 2017, **245**, 747–752.
- 25 19 C. J. Alleyne, A. G. Kirk, W.-Y. Chien and P. G. Charette, Numerical method for high accuracy index of refraction estimation for spectro-angular surface plasmon resonance systems, *Opt. Express*, 2008, **16**(24), 19493–19503.
- 30 20 S. Fillion-Côté, P. J. R. Roche, A. M. Foudeh, M. Tabrizian and A. G. Kirk, Design and analysis of a spectro-angular surface plasmon resonance biosensor operating in the visible spectrum, *Rev. Sci. Instrum.*, 2014, **85**(9), 093107.
- 35 21 K. A. Sochacki, I. A. Shkel, M. T. Record and J. C. Weisshaar, Protein Diffusion in the Periplasm of *E. coli* under Osmotic Stress, *Biophys. J.*, 2011, **100**, 22–31.
- 40 22 D. Dufour, V. Leung and C. M. Lévesque, Bacterial biofilm: structure, function, and antimicrobial resistance, *Endodontic Topics*, 2012, **22**, 2–16.
- 45 23 T. Møretrø, L. Vestby, L. Nesse, S. Storheim, K. Kotlarz and S. Langsrud, Evaluation of efficacy of disinfectants against Salmonella from the feed industry, *J. Appl. Microbiol.*, 2009, **106**(3), 1005–1012.
- 50 24 S. Chambers, B. Peddie and A. Pithie, Ethanol disinfection of plastic-adherent micro-organisms, *J. Hosp. Infect.*, 2006, **63**(2), 193–196.
- 55 25 W. Sopwith, T. Hart and P. Garner, Preventing infection from reusable medical equipment: A systematic review, 2002, **2**(4). **Q4**
- 26 C.-T. Yang, R. Méjard, H. J. Griesser, P. O. Bagnaninchi and B. Thierry, Cellular Micromotion Monitored by Long-Range Surface Plasmon Resonance with Optical Fluctuation Analysis, *Anal. Chem.*, 2015, **87**, 1456–1461.
- 27 R. Robelek and J. Wegener, Label-free and time-resolved measurements of cell volume changes by SPR spectroscopy, *Biosens. Bioelectron.*, 2010, **25**(5), 1221–1224.
- 28 A. K. Epstein, B. Pokroy, A. Seminara and J. Aizenberg, Bacterial biofilm shows persistent resistance to liquid wetting and gas penetration, *Proc. Natl. Acad. Sci. U. S. A.*, 2011, **108**(3), 995–1000.
- 29 I. Gomes, M. Simões and L. Simões, The effects of sodium hypochlorite against selected drinking water-isolated bacteria in planktonic and sessile states, *Sci. Total Environ.*, 2016, **565**, 40–48.